Preprints.org

Article

Not peer-reviewed version

# Characterization of Extracellular Vesicle Cargo in the Experimental Rat Model of Pulmonary Hypertension

Melinee D'Silva , Christina Signoretti , Monika Dzieciatkowska , Angelo D'Alessandro , Michael S. Wolin , Sachin A. Gupte *

Posted Date: 18 September 2026

Keywords: proteomics; lung; disease; flow cytometry; blood coagulation; fibrosis; angiogenesis; redox; reactive oxygen species; MitoSOX

Preprints.org is a free multidisciplinary platform providing preprint service that is dedicated to making early versions of research outputs permanently available and citable. Preprints posted at Preprints.org appear in Web of Science, Crossref, Google Scholar, Scilit, Europe PMC, OpenAlex.

Copyright: This open access article is published under a Creative Commons CC BY 4.0 license, which permit the free download, distribution, and reuse, provided that the author and preprint are cited in any reuse.

*Preprints.org* (www.preprints.org) | NOT PEER-REVIEWED | Posted: 18 September 2026 doi:10.20944/preprints202609.1607.v1

Disclaimer/Publisher's Note: The statements, opinions, and data contained in all publications are solely those of the individual author(s) and contributor(s) and not of MDPI and/or the editor(s). MDPI and/or the editor(s) disclaim responsibility for any injury to people or property resulting from any ideas, methods, instructions, or products referred to in the content.

*Article*

# Characterization of Extracellular Vesicle Cargo in the Experimental Rat Model of Pulmonary Hypertension

**Functional Mitochondria and Post Transitionally Modified Proteins**

**Melinee D'Silva [1] Christina Signoretti [1], Monika Dzieciatkowska [2], Angelo D'Alessandro [2], Michael S. Wolin [3] and Sachin A. Gupte [1,*]**

[1] Department of Pharmacology, New York Medical College, Valhalla, NY 10595
[2] Department of Biochemistry and Molecular Genetics, University of Colorado Anschutz Medical Campus, Aurora, CO, USA
[3] Department of Cell and Molecular Physiology, New York Medical College, Valhalla, NY 10595
* Correspondence: s_gupte@nymc.edu or sachin_gupte@yahoo.com

**Abstract**

Extracellular vesicles (EVs) released by cells carry a diverse molecular cargo, including proteins, lipids, nucleic acids, and mitochondria. In addition, EVs carry antioxidants and free radical producing enzymes like NADPH oxidases or other oxidases. Growing evidence suggests that EV cargo plays a critical role in intercellular communication and disease pathogenesis. In pulmonary hypertension (PH), circulating EV levels are elevated and can alter the function of recipient cells; however, whether EVs transmit functional mitochondria and the composition of their protein cargo remain poorly understood. To address this knowledge gap, we characterized the cargo of EVs in a rat model of Sugen5416 (SU; 20 mg/kg, i.p.)- and hypoxia (10% $O_2$)-induced PH. EVs were isolated from blood collected from the left ventricles of SU/hypoxia (SU/Hx) and SU/normoxia (SU/Nx) rats and analyzed using quantitative mass spectrometry–based proteomics and flow cytometry. Proteomic profiling revealed that EVs contain proteins involved in coagulation, complement and immune signaling, metabolism, receptor signaling, and cytoskeletal organization. Although EVs from SU/Hx rats exhibited an overall decrease in protein abundance, specific proteins involved in cytoskeletal structure, metabolism, immune signaling, and cell adhesion were preferentially enriched and contained reactive oxygen species-dependent and redox-sensitive post-translational modifications, implicating these molecular changes in mechanisms underlying PH progression. Importantly, EVs from SU/Hx rats contained a significantly greater abundance of functionally active mitochondria, as determined by the MitoTracker Red-to-MitoTracker Green signal ratio, while exhibiting lower levels of mitochondrial superoxide anions, as determined by MitoSOX fluorescence. Together, these findings demonstrate, for the first time, that EVs released from the pulmonary circulation in PH can transmit functional mitochondria and biologically active protein cargo capable of modulating vascular and systemic cellular responses.

**Keywords:** proteomics; lung; disease; flow cytometry; blood coagulation; fibrosis; angiogenesis; redox; reactive oxygen species; MitoSOX

---

Microparticles (MPs) and extracellular vesicles (EVs) are cargos involved in cell-to-cell communication [1,2]. MPs and EVs are released through exocytosis, direct plasma membrane budding, and apoptotic body formation [1–3]. These vesicles transport a variety of biological materials, including mitochondria, RNA, DNA, lipids, and proteins. In addition, EVs carry antioxidants, reactive oxygen species (ROS), including superoxide and other free radicals, and/or free radical producing enzymes like NADPH oxidases or other oxidases [4]. Under disease conditions, they deliver biological and signaling molecules from diseased donor cells to healthy recipient cells, where they can trigger inflammation, alter cellular phenotype, reprogram metabolism, and affect

© 2026 by the author(s). Distributed under a Creative Commons CC BY license.

Preprints.org (www.preprints.org) | NOT PEER-REVIEWED | Posted: 18 September 2026 doi:10.20944/preprints202609.1607.v1



numerous cellular functions. In pulmonary hypertension (PH), EVs derived from both lung and non-lung cells have been shown to play pathological roles by transmitting biomolecules that promote disease initiation and progression [5].

EVs originate from several pulmonary cell-types, including pulmonary artery endothelial cells, pulmonary venous endothelial cells, pulmonary artery smooth muscle cells, and platelets [5). Pulmonary microvascular endothelial cells release EVs enriched with cAMP, forming an additional compartment for cAMP signaling [6]. Endothelial-derived EVs from scleroderma-associated PH patients increase endothelial inflammation [7]. Our laboratory previously demonstrated that EVs from scleroderma- and idiopathic-PH patients carry DNA methyltransferases (DNMTs) and ten eleven translocation demethylases (TETs), and that inflammatory cytokine expression negatively correlates with reduced TET3 levels [8]. Additionally, MPs/EVs from late-stage PH (Sugen5416/Hypoxia/Normoxia) rats induce ICAM-1 expression, an important mediator of immune activation and inflammation, in pulmonary artery endothelial cells [9]. EVs expressing CD62P, CD144, and CD235a from idiopathic and chronic thromboembolic PH patients have also been shown to transmit P-selectin glycoprotein ligand-1 and activate transcription and translation of VEGF-A and FGF in human pulmonary artery endothelial cells [10]. Furthermore, EVs derived from human mesenchymal stromal cells (MSCs) have been shown to prevent and even reverse monocrotaline-induced PH in mice, improve mitochondrial function, and repair hypoxia- and Sugen5416/hypoxia-induced injury in pulmonary vessels and pulmonary artery smooth muscle cells in rodent PH models [11,12]. Despite this growing body of research, our understanding of the proteins and organelles carried specifically by EVs in PH remains incomplete.

Given the importance of EVs in transmitting biomolecules from diseased donor cells to recipient cells, we performed unbiased quantitative mass spectrometry–based proteomic profiling and flow cytometry to characterize the biological functions of EV proteins and quantify mitochondrial content in EVs isolated from blood drained from the left ventricle, reflecting lung-derived and non-lung-derived venous return, in control and Sugen5416/Hypoxia/Normoxia PH (SU/Hx) rats. Intriguingly, our findings reveal that EVs from PH rats carry a higher abundance of functionally active mitochondria, as well as both unmodified and post-translationally modified (PTM) cytoskeletal, signaling, cell adhesion, complement, immune proteins, and metabolic enzymes with modifications potentially associated with redox signaling mechanisms contributing to PH development.

## 1. Materials and Methods

**Animal:** All animal procedures were approved by the New York Medical College Institutional Animal Care and Use Committee (A33362-01) and conducted in accordance with the National Institutes of Health Guide for the Care and Use of Laboratory Animals. Age- and weight-matched Sprague–Dawley (SD) rats (n = 5–6 per treatment group) were randomly assigned to receive a subcutaneous injection of Sugen5416 (SU: 20 mg/kg in DMSO). Rats were then maintained either in normoxia (Nx: 21% $O_2$; ambient conditions) for 8 weeks or in hypoxia (Hx: 10% $O_2$) for 3 weeks, followed by normoxia for an additional 5 weeks, as previously described [13]. At the end of the exposure period, rats were euthanized, and blood was collected from the left ventricle for proteomic and flow cytometry analyses.

**Extracellular Vesicles Extraction:** The EVs were extracted from plasma by Total Exosome Isolation kit (Cat# 4484450**;** Thermo Fisher Scientific; https://documents.thermofisher.com/TFS-Assets/CMD/posters/Exosome-poster-ISEV-2013-Boston.pdf) and confirmed by ultracentrifugation methods as previously published [8). Rat plasma samples were collected and immediately placed on ice. Samples were centrifuged at 2000 × g for 20 minutes at 4 °C, and the resulting supernatant (clarified plasma) was carefully transferred to fresh tubes without disturbing the pellet and kept on ice. Clarified plasma was then transferred to a new microcentrifuge tube and mixed with 0.5 volumes of 1× PBS, followed by thorough vortexing to ensure homogeneity. Next, 0.2 volumes of Exosome Precipitation Reagent for plasma were added based on the total plasma–PBS volume (e.g., 100 µL plasma + 50 µL PBS + 30 µL Exosome Precipitation Reagent). The mixture was vortexed or gently inverted until a cloudy suspension formed, then incubated at room temperature for 10 minutes and

© 2026 by the author(s). Distributed under a Creative Commons CC BY license.

Preprints.org (www.preprints.org) | NOT PEER-REVIEWED | Posted: 18 September 2026 doi:10.20944/preprints202609.1607.v1



centrifuged at 10,000 × g for 5 minutes at room temperature. After centrifugation, the supernatant was discarded without disturbing the exosome-containing pellet. The pellet was resuspended in PBS, with the resuspension volume adjusted according to the initial plasma volume. EVs were used immediately for downstream applications or stored at −20 °C for later use.

**Flow Cytometry:** To evaluate the alterations in mitochondrial membrane potential and matrix superoxide levels reported in the study, mitochondrial membrane potential and mitochondrial superoxide production was quantified using MitoTracker dyes and MitoSOX, respectively, and analyzed by flow cytometry as previously described [14]. Extracted EVs resuspended in PBS were incubated for 15–30 minutes at 4 °C with either MitoTracker Green (FITC) (ThermoFisher, Cat# M7514), MitoTracker Red FM (APC) (ThermoFisher, Cat# M22425), MitoSOX (ThermoFisher, Cat# M360007) or PE-CD63 antibody (Miltenyi Biotec, Cat# 130-129-816) in the dark, according to the manufacturers' recommendations. After staining, samples were washed twice with 2 mL of FCS buffer at 400 × g for 10 minutes at 4 °C. The resulting pellets were resuspended in 300 µL of FCS buffer and loaded onto the flow cytometer. An unstained control was run first to establish system parameters, followed by compensation controls and stained samples for each group. The resulting compensation matrix was applied to all samples. Flow Cytometry Standard (.fcs) files were exported and analyzed using FlowJo (version 11). EVs were gated based on relative compensation, and analytes were reported when signal intensities met the predefined gating criteria compared with the unstained control.

**Proteomics:** Proteins from resuspended EV preparations (300 µg/mL total protein) were analyzed by mass spectrometry-based proteomics at the University of Colorado. Proteomic workflows followed previously published methods [15,16].

10 ug of samples were mixed with 5% SDS in 100 mM triethylammonium bicarbonate (TEAB), pH 7.5, lysis buffer. Protein digestion was performed using a 96-well S-Trap plate (Protifi, Huntington, NY) following the manufacturer's protocol. Samples were reduced with 10 mM DTT at 55 °C for 30 min, cooled to room temperature, and alkylated with 25 mM iodoacetamide in the dark for 30 min. A final concentration of 1.2% phosphoric acid was then added, followed by six volumes of binding buffer (90% methanol, 100 mM TEAB, pH 7.1). After gentle mixing, the protein mixtures were loaded onto the 96-well S-Trap plate, centrifuged at 1500 × g for 2 min, and the flow-through was collected and reloaded. This loading step was repeated three times. The plate was then washed three times with 300 µL of binding buffer.

For digestion, 1 µg of sequencing-grade trypsin (Promega) and 125 µL of digestion buffer (50 mM TEAB) were added to each well, and samples were incubated at 37 °C for 6 h. Peptides were eluted sequentially using three buffers — 50 mM TEAB, 0.2% formic acid in water, and 50% acetonitrile with 0.2% formic acid — each applied in 100 µL volumes and repeated once. All eluates were pooled, lyophilized, and resuspended in 200 µL of 0.1% formic acid. A 20 ul of each sample was loaded onto individual Evotips for desalting and then washed with 20 µL 0.1% FA followed by the addition of 100 µL storage solvent (0.1% FA) to keep the Evotips wet until analysis. The Evosep One system (Evosep, Odense, Denmark) was used to separate peptides on a Pepsep column, (150 um inter diameter, 15 cm) packed with ReproSil C18 1.9 um, 120A resin. The system was coupled to the timsTOF Pro mass spectrometer (Bruker Daltonics, Bremen, Germany) via the nano-electrospray ion source (Captive Spray, Bruker Daltonics). The mass spectrometer was operated in parallel accumulation–serial fragmentation (PASEF) mode with a ramp time of 100 ms, acquiring 10 PASEF MS/MS scans per topN acquisition cycle. MS/MS spectra were recorded over an m/z range of 100–1700, with ion mobility scanned from 0.7 to 1.50 Vs/cm². Precursors were isolated within ±1 Th and fragmented using ion mobility–dependent collision energies linearly ramped from 20 to 59 eV in positive ion mode. Low-abundance precursor ions with intensities >500 counts but below a target intensity of 20,000 counts were rescheduled for repeated fragmentation; all other ions were dynamically excluded for 0.4 min.

Raw data files were converted to MGF peak lists, and all downstream identification, validation, filtering, and quantification steps were performed using FragPipe version 13.0. Database searching was carried out with MSFragger version 3.0 against a rat protein database supplemented with decoys

© 2026 by the author(s). Distributed under a Creative Commons CC BY license.

Preprints.org (www.preprints.org) | NOT PEER-REVIEWED | Posted: 18 September 2026 doi:10.20944/preprints202609.1607.v1



and common contaminants. Search parameters were set as follows: enzyme specificity — trypsin, fully specific, allowing up to two missed cleavages; precursor isotope error tolerance up to two isotopic peaks; mass tolerances — 15.0 ppm for MS1 and 0.04 Da for MS2. Carbamidomethylation of cysteine (+57.021464 Da) was included as a fixed modification. Variable modifications included oxidation of methionine (+15.994915 Da), hydroxylation of proline (+15.994915 Da), protein N-terminal acetylation (+42.010565 Da), and pyroglutamate formation from N-terminal glutamine or cysteine (−17.026549 Da).

**Statistical analysis:** All statistical analyses and generated figures were created using GraphPad Prism 5.0 Software. Technical replicates were used in all assays and averaged together. All data underwent outlier tests, and outliers were removed as necessary (Robust regression, Outlier removal Q=1%). All values in the figures are the mean ± SD. N is number of rats per group.

## 2. Results:

**$CD63^+$ EVs are increased in pulmonary hypertension:** As expected, SU/Hx significantly reduced the pulmonary artery acceleration time-to-ejection time (PAAT-to-ET) ratio compared with SU/Nx controls (Figure 1A). Decreased PAAT-to-ET ratio is associated with the increased pulmonary arterial pressure [17]. Consistent with these hemodynamic changes, SU/Hx rats also exhibited cardiac remodeling (Table 1). The combination of increased interventricular septal thickness (IVS) during both diastole and systole together with the reduced PAAT/ET ratio confirms the development of SU/Hx-induced PH. $CD63^+$ is highly enriched on the surface of EVs and is widely used as a marker for EVs. Forward- and side-scatter flow-cytometry analyses demonstrated a significant increase in $CD63^+$ EV in blood collected from the left ventricle of SU/Hx rats compared with SU/Nx rats (Figure 1B–D).

**Table 1. Echocardiographic assessment of left ventricular geometry and function in SU/Nx and SU/Hx groups.**

| | SU/Nx | N | SU/Hx | N | P value vs SU/Nx |
|---|---|---|---|---|---|
| $IVS_d$ (mm) | 1.97±0.26 | 4 | 2.54±0.25 | 4 | 0.036 |
| $IVS_s$ (mm) | 3.58±0.39 | 4 | 4.20±0.14 | 4 | 0.024 |
| $LVID_d$ (mm) | 8.49±0.31 | 5 | 8.87±0.40 | 4 | 0.133 |
| $LVID_s$ (mm) | 4.07±0.47 | 4 | 5.03±0.79 | 4 | 0.001 |
| $LVPW_d$ (mm) | 1.65±0.16 | 4 | 2.27±0.21 | 4 | 0.025 |
| $LVPW_s$ (mm) | 3.53±0.38 | 4 | 3.68±0.25 | 4 | 0.528 |

Values represent mean ± SEM for interventricular septal thickness at diastole (IVSd) and systole (IVSs), left ventricular internal diameter at diastole (LVIDd) and systole (LVIDs), and left ventricular posterior wall thickness at diastole (LVPWd) and systole (LVPWs). Comparisons between SU/Nx and SU/Hx groups were performed using unpaired two-tailed t-tests. $P < 0.05$ was considered statistically significant.

© 2026 by the author(s). Distributed under a Creative Commons CC BY license.

Preprints.org (www.preprints.org) | NOT PEER-REVIEWED | Posted: 18 September 2026 doi:10.20944/preprints202609.1607.v1



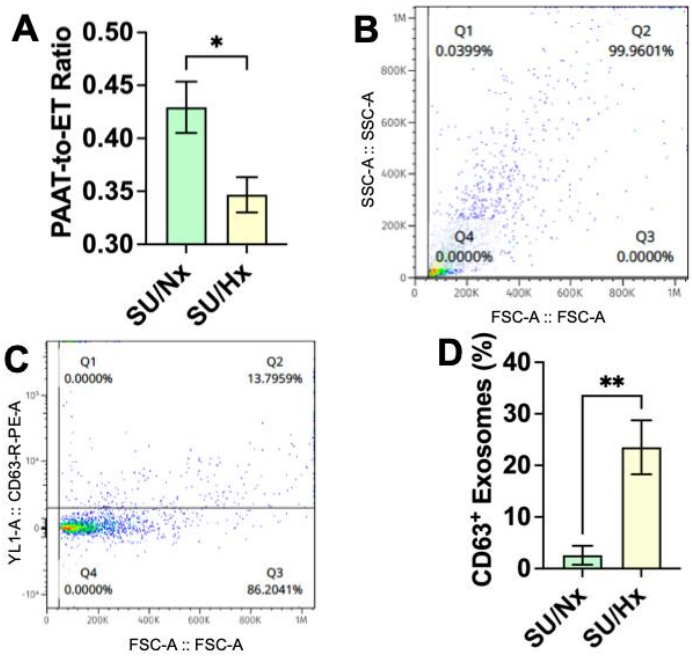


**Figure 1. Hypoxia alters the release and characteristics of CD63⁺ EVs.** This figure compares circulating EVs isolated from rats with Sugen-induced pulmonary hypertension maintained under normoxic (SU/Nx) or hypoxic (SU/Hx) conditions. (A) Pulmonary Artery Acceleration Time–to–Ejection Time (PAAT/ET) ratio, a Doppler-based measure of pulmonary hemodynamics, is significantly reduced in SU/Hx rats compared with SU/Nx controls (*$p < 0.05$; n=5), consistent with severe pulmonary hypertension. (B) Forward Scatter-Area (FSC-A) versus Side Scatter-Area (SSC-A) flow-cytometry plots display the size and granularity of isolated extracellular vesicles, with 99.96% of events localized within the expected EVs gate (Q2). (C) CD63 fluorescence (YL1-A::CD63-R-PE-A) plotted against FSC-A identifies CD63⁺ EVs in Q3, representing 86.20% of total events. (D) Quantification of CD63⁺ EVs show a significantly higher proportion of CD63⁺ particles in the SU/Hx group compared with SU/Nx (**$p < 0.01$; n=5), indicating enhanced EV release under chronic hypoxia.

**Characteristics of proteins identified in CD63⁺ EVs by proteomics:** To characterize the protein cargo of EVs, we performed unbiased proteomic analysis on EVs isolated from the blood of SU/Hx and SU/Nx rats. The volcano plot demonstrated clear differential protein expression between the two groups (Figure 2A). *In silico* analysis using the Panther Classification System identified the biological functions associated with the up- and down-regulated proteins. Overall, proteins from 144 distinct pathways were detected (Figure 2B, C). These pathways included cytoskeletal regulation via Rho GTPase, cadherin signaling, FGF signaling, nicotinic acetylcholine receptor signaling, chemokine- and cytokine-mediated inflammation, integrin signaling, ubiquitin-proteasome processes, and glycolysis. Many of these pathways were significantly altered, either up- or down-regulated, in EVs from SU/Hx rats (Figure 2C).

© 2026 by the author(s). Distributed under a Creative Commons CC BY license.

Preprints.org (www.preprints.org) | NOT PEER-REVIEWED | Posted: 18 September 2026 doi:10.20944/preprints202609.1607.v1



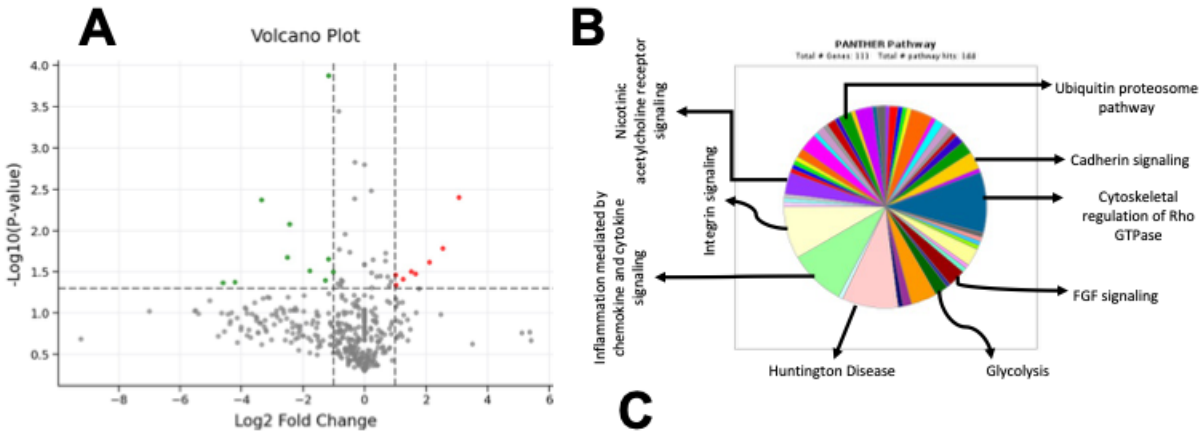


C

| Annotation Version and Release Date: | PANTHER version 19.0 Released 2024-06-20 | | | | | |
|---|---|---|---|---|---|---|
| Analyzed List: | Client Text Box Input (Rattus norvegicus) | | | | | |
| Reference List: | Rattus norvegicus (all genes in database) | | | | | |
| Test Type: | FISHER | | | | | |
| Correction: | FDR | | | | | |
| PANTHER Pathways | Rattus norvegicus - REFLIST (22870) | Client Text Box Input (111) | Client Text Box Input (expected) | Client Text Box Input (fold Enrichment) | Client Text Box Input (raw P-value) | Client Text Box Input (FDR) |
| Cytoskeletal regulation by Rho GTPase | 82 | 14 | 0.4 | 35.18 | 2.88E-18 | 4.64E-16 |
| Huntington disease | 171 | 13 | 0.83 | 15.66 | 2.29E-12 | 1.23E-10 |
| Integrin signaling pathway | 189 | 12 | 0.92 | 13.08 | 1.38E-10 | 5.56E-09 |
| Nicotinic acetylcholine receptor signaling pathway | 92 | 5 | 0.45 | 11.2 | 8.65E-05 | 2.32E-03 |
| Glycolysis | 56 | 3 | 0.27 | 11.04 | 2.56E-03 | 4.12E-02 |
| Inflammation mediated by chemokine and cytokine signaling pathway | 249 | 13 | 1.21 | 10.76 | 2.58E-10 | 8.30E-09 |
| Ubiquitin proteasome pathway | 65 | 3 | 0.32 | 9.51 | 3.91E-03 | 4.84E-02 |
| Cadherin signaling pathway | 123 | 4 | 0.6 | 6.7 | 3.06E-03 | 4.48E-02 |
| FGF signaling pathway | 127 | 4 | 0.62 | 6.49 | 3.44E-03 | 4.61E-02 |

**Figure 2. Proteomic profiling and pathway enrichment analysis of EV cargo.** (A) Volcano plot depicting differentially expressed EV proteins. The x-axis represents $\log_2$ fold change (SU/Hx vs. SU/Nx; $n = 5$), and the y-axis represents $-\log_{10}(P \text{ value})$. Proteins significantly upregulated in SU/Hx rats are shown on the right (red), while significantly downregulated proteins are shown on the left (green). Proteins that do not meet significance thresholds are shown in gray. (B–C) PANTHER pathway enrichment analysis (version 19.0; *Rattus norvegicus* database) of differentially expressed EV proteins. Enriched pathways include cytoskeletal regulation by Rho GTPase, Huntington disease, integrin signaling, chemokine/cytokine-mediated inflammation, cadherin signaling, glycolysis, nicotinic acetylcholine receptor signaling, ubiquitin–proteasome pathways, and FGF signaling. Ranked pathway enrichment analysis was performed using Fisher's exact test with false discovery rate (FDR) correction, highlighting the most significantly altered functional pathways in SU/Hx-derived EVs. Collectively, these findings demonstrate that chronic hypoxia profoundly alters signaling, metabolic, and structural pathways within EV protein cargo.

**Expression levels and biological functions of differentially regulated proteins in the EVs of rats with pulmonary hypertension:** While total EVs protein content did not differ between the two groups (Figure 3A); proteins, including those involved in blood coagulation, were reduced in EVs from SU/Hx rats compared with SU/Nx rats, several key proteins were notably increased. These included: cytoplasmic dynein 1 heavy chain 1, a cytoskeletal motor protein involved in mitosis, intracellular trafficking, and retrograde transport; attractin, a signaling protein associated with inflammatory responses and energy homeostasis; long-chain fatty acid–CoA ligase 1, a metabolic enzyme essential for fatty acid metabolism and β-oxidation; vascular cell adhesion protein 1 (VCAM1), a cell-adhesion molecule that mediates leukocyte binding to vascular endothelial cells; Ig-gamma-2A chain C region, a complement- and immune-related protein; high-mobility group protein B1 (HMGB1), a DNA-binding and chromatin-modifying protein that also functions extracellularly as a potent pro-inflammatory mediator; phosphatidylinositol-glycan-specific phospholipase D (GPI-PLD), an enzyme that cleaves GPI anchors involved in immune activation; haptoglobin, which binds

© 2026 by the author(s). Distributed under a Creative Commons CC BY license.

Preprints.org (www.preprints.org) | NOT PEER-REVIEWED | Posted: 18 September 2026 doi:10.20944/preprints202609.1607.v1



and removes free hemoglobin from the circulation, preventing iron loss and oxidative tissue injury while modulating immune responses; and serine protease inhibitor A3N (Serpin A3N), a neutrophil elastase inhibitor that regulates inflammation and limits tissue damage. All these proteins were elevated in EVs isolated from SU/Hx rats compared with SU/Nx rats (Figures 3B and 4).

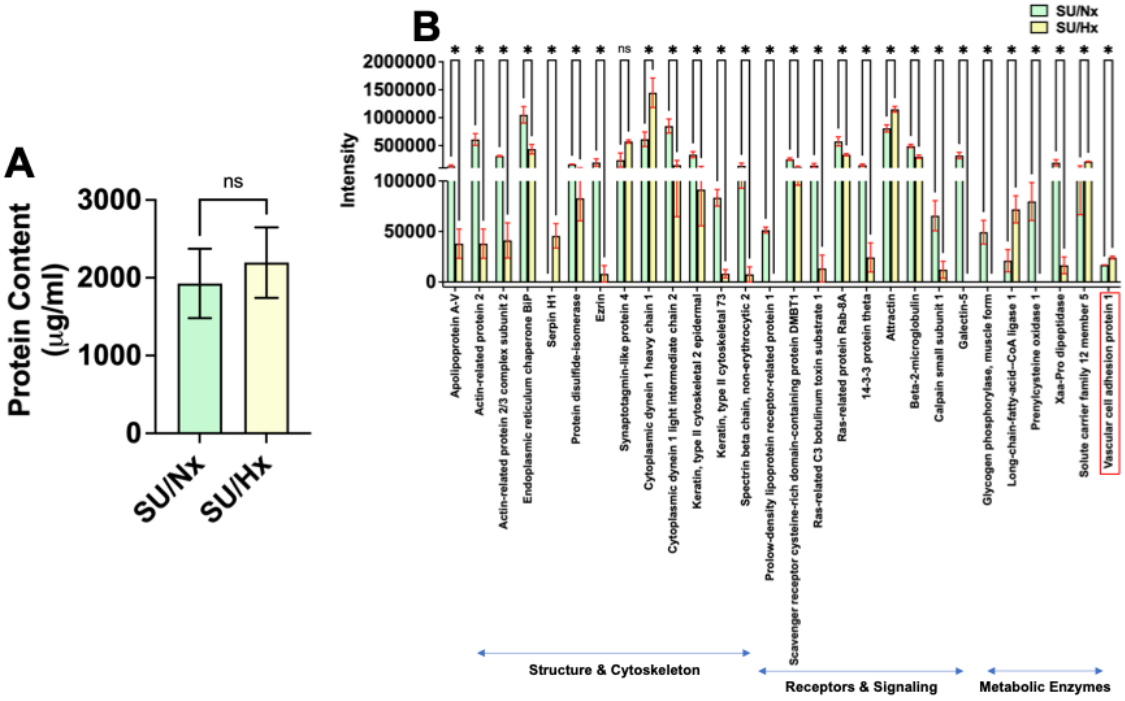


**Figure 3. Differential expression of EV proteins grouped by functional category.** (A) Total EV protein content (µg/mL) does not differ between SU/Nx and SU/Hx groups. (B) The figure displays the abundance of selected EV proteins in SU/Nx (green bars) versus SU/Hx (yellow bars) rats (n=3 each group). Structure & Cytoskeleton: Most cytoskeletal and structural proteins, including Apolipoprotein A-V and Actin-related protein 2/3 complex subunit 2, are reduced in SU/Hx EV. Exceptions include Serpin H1 and cytoplasmic dynein 1 heavy chain 1, which are elevated. Receptors & Signaling: Signaling proteins such as Prolow-density lipoprotein receptor-related protein 1 and Rab-8A are decreased under hypoxia, whereas Attractin is increased. Metabolic Enzymes: Several metabolic enzymes, including long-chain fatty acid–CoA ligase 1, solute carrier family 12 member 5, and vascular cell adhesion protein 1 (VCAM1; in red box), are significantly upregulated in SU/Hx EVs. Collectively, these patterns indicate that hypoxia reshapes the EV proteome, selectively enhancing metabolic, adhesion-related, and stress-responsive protein cargo.

© 2026 by the author(s). Distributed under a Creative Commons CC BY license.

Preprints.org (www.preprints.org) | NOT PEER-REVIEWED | Posted: 18 September 2026 doi:10.20944/preprints202609.1607.v1



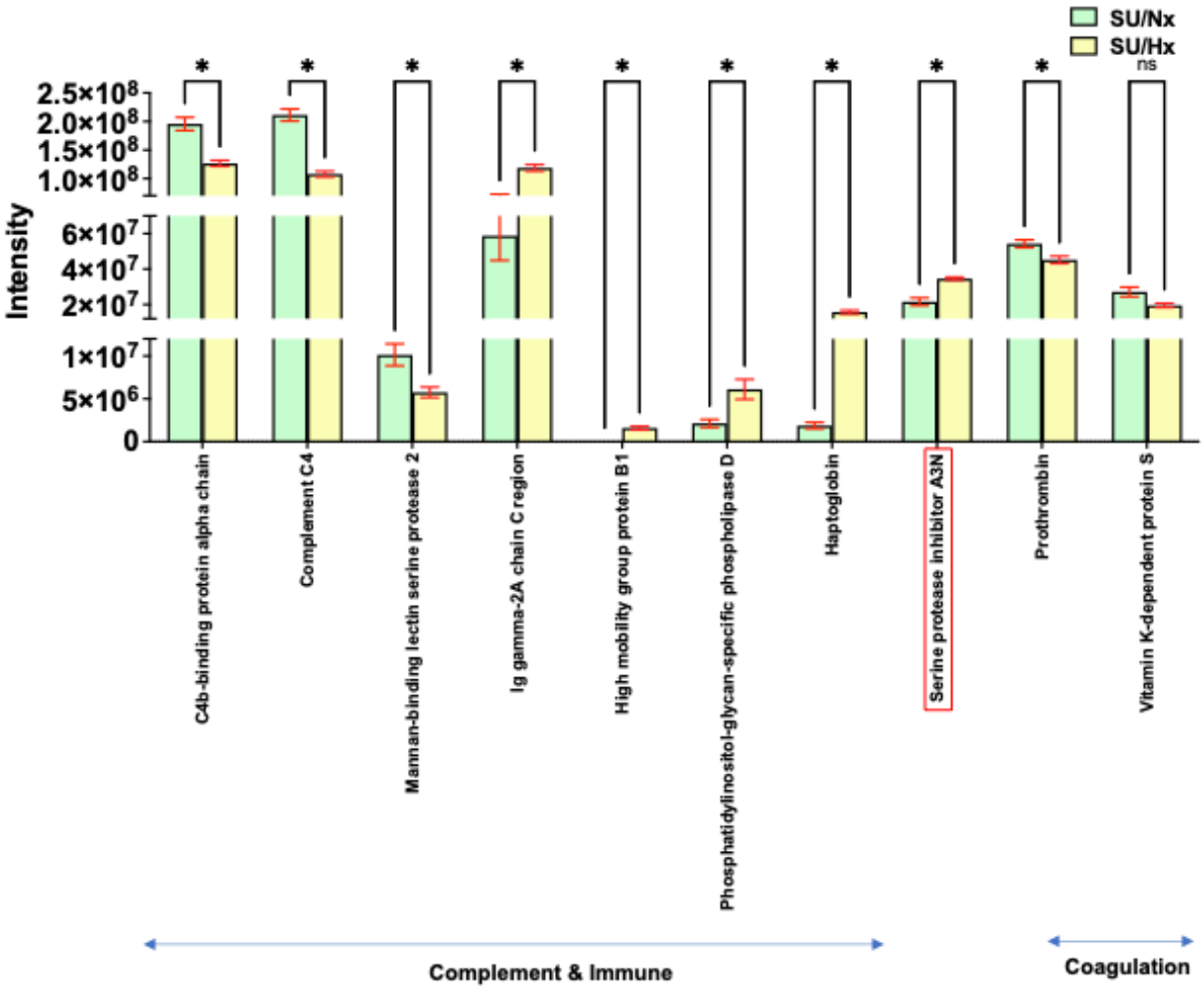


**Figure 4. Biological functions of EV proteins altered in pulmonary hypertension.** This figure illustrates differences in EV proteins associated with immune pathways, complement activation, and the coagulation cascade between SU/Nx (green bars) and SU/Hx (yellow bars) groups (n=3 rats/group). Complement & Immune Proteins: C4b-binding protein $\alpha$-chain, Complement C4, and Mannan-binding lectin serine protease 2 are significantly reduced in SU/Hx EVs. Conversely, Ig-gamma-2A chain C region, phosphatidylinositol-glycan–specific phospholipase D (GPI-PLD), and haptoglobin are elevated (*$p < 0.05$). Coagulation-Related Proteins: Serine protease inhibitor A3N (Serpin A3N), a regulator of neutrophil elastase and inflammation, is significantly increased, whereas prothrombin is decreased in SU/Hx EVs (*$p < 0.05$). Vitamin K-dependent protein S is unchanged. These results indicate that hypoxia-derived EVs carry altered immune, complement, and coagulation protein signatures that may contribute to pulmonary hypertension pathobiology.

**Determination of post-translationally modified proteins in EVs of rats with pulmonary hypertension:** Reactive oxygen species and redox imbalance are common features in the lungs and pulmonary vasculature of both patients and animal models with PH [18]. These redox disturbances are known to induce post-translational modifications (PTM) in proteins. To characterize these modifications within EV cargo, we performed PTM-specific proteomic analysis on EVs isolated from SU/Hx rats. A comprehensive list of the detected modified proteins is provided in Table 2. Notably, oxidation of M (15.9949), N-term acetylation (42.0106), P oxidation (15.9949), Q deamidation (-17.0265), and C carbamidomethylation (57.0215) modifications were commonly observed among lung-associated proteins, whereas C (57.0215) modifications predominated in proteins from non-lung tissues. Expression levels of these modified proteins in SU/Hx versus SU/Nx groups are presented in Figure 5 and Table 2, while their corresponding biological functions are summarized in Table 3.

© 2026 by the author(s). Distributed under a Creative Commons CC BY license.

Preprints.org (www.preprints.org) | NOT PEER-REVIEWED | Posted: 18 September 2026 doi:10.20944/preprints202609.1607.v1



**Table 2. List of modified proteins.**

| Peptide Sequence | Modified Sequence | Prev AA | Next AA | Assigned Modification | Entry Name | SU/Hx | SU/Nx | T.Test (P=) |
|---|---|---|---|---|---|---|---|---|
| | | | | | | Spectral Intensity (Mean±SEM) | | SU/Hx Vs SU/Nx |
| FDHPFIFMIVESETQSPLFVGK | FDHPFIFM[15.9949]IVESETQSPLFVGK | K | V | 8M(15.9949) | A1AT | 136606.6 ± 10284.5 | 40959.0 ± 14988.5 | 0.008 |
| YVRETGLMAFTNLK | YVRETGLM[15.9949]AFTNLK | R | I | 8M(15.9949) | A1I3 | 111713.0 ± 19247.1 | 16381.6 ± 18692.8 | 0.01 |
| AEQGAYLGPLPYKGGENCIK | AEQGAYLGPLPYKGGENC[57.0215]IK | K | A | 18C(57.0215) | A1M | 913418.5 ± 28764.3 | 517110.4 ± 167803.2 | 0.006 |
| YPIEHGIITNWDDMEK | YPIEHGIITNWDDM[15.9949]EK | K | I | 14M(15.9949) | ACTC | 0.0 ± 0.0 | 55061.7 ± 156081.0 | 0.003 |
| LECGGGRWGNK | LEC[57.0215]GGGRWGNK | K | G | 3C(57.0215) | AL1A7 | 32940.5 ± 5312.8 | 7625.3 ± 5926.9 | 0.026 |
| HPYFYAPELLYYAEKYNEVLTQCCTESDKAACLTPK | HPYFYAPELLYYAEKYNEVLTQC[57.0215]C[57.0215]TESDKAAC[57.0215]LTPK | R | L | 23C(57.0215), 24C(57.0215), 32C(57.0215) | ALBU | 572055.3 ± 14735.1 | 245660.2 ± 94774.6 | 0.012 |
| VAGLMEDTFPGLLGLHVLR | VAGLM[15.9949]EDTFPGLLGLHVLR | R | L | 5M(15.9949) | ALS | 492089.7 ± 39390.6 | 311142.6 ± 72479.3 | 0.035 |
| GVKGEECQLCEVENR | GVKGEEC[57.0215]QLC[57.0215]EVENR | K | Y | 7C(57.0215), 10C(57.0215) | ATRN | 175892.3 ± 18153.2 | 64310.3 ± 88709.8 | 0.01 |
| KLMQCLPNSNDVK | KLM[15.9949]QC[57.0215]LPNSNDVK | K | M | 3M(15.9949), 5C(57.0215) | C4BPA | 1850638.4 ± 219250.6 | 3284065.2 ± 1025182.3 | 0.003 |
| LEAVSHTSDMHCGYGDSPSK | LEAVSHTSDMHC[57.0215]GYGDSPSK | R | G | 12C(57.0215) | CAP1 | 26774.2 ± 26805.9 | 268926.2 ± 962775.3 | 0.040 |
| ADSRDPASDQMK | n[42.0106]ADSRDPASDQMK | M | Q | N-term(42.0106) | CATA | 28619.5 ± 7583.2 | 65682.1 ± 90735.4 | 0.03 |
| FFTHEPQDIHHFSPMGFPHK | FFTHEPQDIHHFSPM[15.9949]GFPRHK | R | R | 15M(15.994) | CLUS | 97640.0 ± 21276.4 | 322427.5 ± 90617.4 | 0.013 |
| SCGLFGLR | SC[57.0215]GLFGLR | R | R | 2C(57.0215) | CO4 | 55659.0 ± 55724.9 | 495874.1 ± 79118.5 | 0.0034 |
| LSVQSSPECIVGK | LSVQSSPEC[57.0215]IVGK | R | F | 9C(57.0215) | F13A * | 42027.2 ± 5540.7 | 151781.9 ± 117542.4 | 0.006 |
| ATCYEDRGLSYRGQAK | ATC[57.0215]YEDRGLSYRGQAK | K | T | 3C(57.0215) | FA12 | 39461.2 ± | 6707.1 ± | 0.007 |

© 2026 by the author(s). Distributed under a Creative Commons CC BY license.

Preprints.org (www.preprints.org) | NOT PEER-REVIEWED | Posted: 18 September 2026 doi:10.20944/preprints202609.1607.v1



| | | | | | | | | |
|---|---|---|---|---|---|---|---|---|
| | | | | | | 4022.7 | 48763.9 | |
| GECPWQAVLK | GEC[57.0215]PWQAVLK | K | F | 3C(57.0215) | FA7 * | 48982.4 ± 2244.5 | 32889.6 ± 9436.4 | 0.004 |
| WIVTAAHCLKPGDKIEVVAGEHNIDEK | WIVTAAHC[57.0215]LKPGDKIEVVAGEHNIDEK | K | E | 8C(57.0215) | FA9 | 32669.2 ± 2133.9 | 86590.2 ± 18462.8 | 0.004 |
| IQCAAGYEQSEHNVCQDIDECTSGTHNCR | IQC[57.0215]AAGYEQSEHNVC[57.0215]QDIDEC[57.0215]TSGTHNC[57.0215]R | L | | 3C(57.0215), 15C(57.0215), 21C(57.0215), 28C(57.0215) | FBLN3 * | 44539.0 ± 8489.3 | 86205.4 ± 8288.5 | 0.009 |
| KIHSMCPDCPHPVDLSAPSVLEAATESLAK | KIHSMC[57.0215]PDC[57.0215]PHPVDLSAPSVLEAATESLAK | R | F | 6C(57.0215), 9C(57.0215) | FETUB | 1863312.2 ± 250696.1 | 723245.5 ± 211607.5 | 0.007 |
| YCGLPGEYWLGNDK | YC[57.0215]GLPGEYWLGNDK | K | I | 2C(57.0215) | FIBB | 857750.2 ± 132669.5 | 1724095.9 ± 327436.5 | 0.003 |
| LTCQCLGFGSGHFR | LTC[57.0215]QC[57.0215]LGFGSGHFR | C | | 3C(57.0215), 5C(57.0215) | FINC * | 160109.9 ± 25187.7 | 364027.1 ± 434512.4 | 0.006 |
| GNTFSCSCPAPFSGSR | GNTFSC[57.0215]SC[57.0215]PAPFSGSR | R | C | 6C(57.0215), 8C(57.0215) | HABP2 | 45378.9 ± 970.3 | 60261.9 ± 14033.0 | 0.009 |
| ELGSPPGISLDTIDAAFSCPGSSK | ELGSPPGISLDTIDAAFSC[57.0215]PGSSK | K | L | 19C(57.0215) | HEMO * | 969130.7 ± 152997.2 | 355985.3 ± 107917.3 | 0.01 |
| TSCLLFMGR | TSC[57.0215]LLFMGR | R | V | 3C(57.0215) | HEP2 | 597736.9 ± 49749.8 | 470523.4 ± 66491.2 | 0.04 |
| VMPICLPSKDYVAPGR | VMPIC[57.0215]LPSKDYVAPGR | K | M | 5C(57.0215) | HPT * | 735273.0 ± 34582.4 | 8983.0 ± 6359.5 | 1.76E-05 |
| THEIGCPPPPEGKDNSDRPPLQEGALPQMLPGHSGPSGTNR | THEIGC[57.0215]PPPPEGKDNSDRPPLQEGALPQMLPGHSGPSGTNR | K | S | 6C(57.0215) | HRG | 27724.8 ± 6073.6 | 0.0 ± 6359.5 | 0.005 |
| RLEMYCAPLKPTK | RLEMYC[57.0215]APLKPTK | R | S | 6C(57.0215) | IGF1 * | 43296.1 ± 3043.7 | 71055.4 ± 11962.4 | 0.025 |
| GPQVYTMAPPKEEMTQSQVSITCMVK | GPQVYTMAPPKEEM[15.9949]TQSQVSITC[57.0215]M[15.9949]VK | R | G | 14M(15.9949), 23C(57.0215), 24M(15.9949) | IGG2A * | 86802.0 ± 3924.3 | 0.0 ± 23288.7 | 1.2E-05 |
| DSTYSMSSTLSLTKADYESHNLYTCEVVHKTSSSPVVK | DSTYSMSSTLSLTKADYESHNLYTC[57.0215]EVVHKTSSSPVVK | K | S | 25C(57.0215) | KACB * | 46037.0 ± 4201.5 | 5570.0 ± 25443.9 | 0.002 |

© 2026 by the author(s). Distributed under a Creative Commons CC BY license.

Preprints.org (www.preprints.org) | NOT PEER-REVIEWED | Posted: 18 September 2026 doi:10.20944/preprints202609.1607.v1



| | | | | | | | | |
|---|---|---|---|---|---|---|---|---|
| TGAISGHSLKQCGHQLSACHQDIYEGLDMR | TGAISGHSLKQC[57.0215]GHQLSAC[57.0215]HQDIYEGLDMR | R | G | 12C(57.0215), 19C(57.0215) | KLKB1 | 34646.9 ± 7215.5 | 5056.6 ± 4766.3 | 0.01 |
| VQEERDPGNEQGPIHGHGWLHAK | VQEERDPGNEQGP[15.9949]IHGHGWLHAK | R | Q | 13P(15.9949) | KNG1 * | 54112.6 ± 3354.5 | 2955.3 ± 3767.8 | 0.0002 |
| QGFQCQVCCFVVHK | Q[-17.0265]GFQC[57.0215]QVC[57.0215]C[57.0215]FVVHK | K | R | 1Q(-17.0265), 5C(57.0215), 8C(57.0215), 9C(57.0215) | KPCA | 32634.1 ± 5978.2 | 12580.8 ± 5599.9 | 0.046 |
| GQYEFHSLEIQSCQLR | GQYEFHSLEIQSC[57.0215]QLR | R | G | 13C(57.0215) | LBP | 0.0 ± 0.0 | 25186.5 ± 6462.2 | 0.002 |
| TSLGDSVPCDHYCHNYLGGYYCSCR | TSLGDSVP[15.9949]C[57.0215]DHYC[57.0215]HNYLGGYYC[57.0215]SC[57.0215]R | R | V | 8P(15.9949), 9C(57.0215), 13C(57.0215), 22C(57.0215), 24C(57.0215) | MASP2 * | 0.0 ± 0.0 | 48617.9 ± 7971.7 | 5.2E-06 |
| FQGTSYNSCTTEGR | FQGTSYNSC[57.0215]TTEGR | R | T | 9C(57.0215) | MMP2 | 47053.1 ± 4339.1 | 11530.9 ± 13872.1 | 0.02 |
| KLFDELVVDKDLFHCLSFTIPR | KLFDELVVDKDLFHC[57.0215]LSFTIPR | R | L | 15C(57.0215) | MUG1 * | 13602060.7 ± 620174.5 | 4637864.8 ± 1711132.1 | 0.002 |
| QIATLHAQVTDMK | Q[-17.0265]IATLHAQVTDMK | K | K | 1Q(-17.0265) | MYH9 * | 173373.4 ± 14893.1 | 35936.2 ± 1704545.6 | 0.002 |
| VATLPPSTQETGGQLLCR | VATLPPSTQETGGQLLC[57.0215]R | R | T | 17C(57.0215) | PCSK9 * | 53239.8 ± 16979.5 | 123264.4 ± 31974.3 | 0.023 |
| ASPEESDGDLSCVCVK | ASPEESDGDLSC[57.0215]VC[57.0215]VK | R | T | 12C(57.0215), 14C(57.0215) | PLF4 | 28720.5 ± 21234.7 | 144189.7 ± 26454.2 | 0.006 |
| QLAAGSIADCLAKCEGETDFICR | Q[-17.0265]LAAGSIADC[57.0215]LAKC[57.0215]EGETDFIC[57.0215]R | K | S | 1Q(-17.0265), 10C(57.0215), 14C(57.0215), 22C(57.0215) | PLMN | 42607.8 ± 910.3 | 11305.9 ± 43455.8 | 0.003 |
| VCFELFADK | VC[57.0215]FELFADK | R | V | 2C(57.0215) | PPIA | 27169.8 ± 13601.7 | 79040.2 ± 23576.0 | 0.03 |
| FCQQEMGFQDCR | FC[57.0215]QQEM[15.9949]GFQDC[57.0215]R | R | V | 2C(57.0215), 6M(15.9949), 11C(57.0215) | PROC | 46736.7 ± 1885.6 | 10417.6 ± 24460.0 | 0.01 |
| ITENIGCVMTGMTADSR | ITENIGC[57.0215]VMTGMTADSR | K | S | 7C(57.0215) | PSA6 | 28378.6 ± 1773.7 | 8635.9 ± 8586.8 | 0.04 |
| QVSDHIAVYR | Q[-17.0265]VSDHIAVYR | K | Q | 1Q(-17.0265) | SEPP1 | 49516.1 ± 5739.8 | 65654.5 ± 25468.6 | 0.04 |

© 2026 by the author(s). Distributed under a Creative Commons CC BY license.

Preprints.org (www.preprints.org) | NOT PEER-REVIEWED | Posted: 18 September 2026 doi:10.20944/preprints202609.1607.v1



| | | | | | | | | |
|---|---|---|---|---|---|---|---|---|
| IISELRMPK | IISELRM[15.9949]PK | R | F | 7M(15.9949) | SPA3K | 46961.4 ± 4696.1 | 4905.4 ± 3472.8 | 0.002 |
| DSLRPSMIDELYLPK | DSLRPSM[15.9949]IDELYLPK | K | F | 7M(15.9949) | SPA3N | 355578.8 ± 48545.5 | 194021.4 ± 62385.1 | 0.022 |
| EECSIPVCGQEGR | EEC[57.0215]SIPVC[57.0215]GQEGR | R | T | 3C(57.0215), 8C(57.0215) | THRB | 1071264.8 ± 82498.4 | 512697.9 ± 139019.6 | 0.008 |
| EGVCPEGSIDSAPVK | EGVC[57.0215]P[15.9949]EGSIDSARPVK | W | 4C(57.0215), 5P(15.9949) | | TRFE * | 152849.9 ± 13061.3 | 30924.7 ± 29999.5 | 0.011 |
| CGPCKPGYTGDQTR | C[-17.0265]GPC[57.0215]KPGYTGDQTR | R | G | 1C(-17.0265), 4C(57.0215) | TSP4 | 28375.5 ± 4856.6 | 49117.4 ± 20807.7 | 0.030 |
| CLAPDVYPIDRLEIELFKGDR | C[57.0215]LAPDVYPIDRLEIELFKGDR | K | L | 1C(57.0215) | VCAM1 | 24229.3 ± 1341.5 | 5630.5 ± 14785.5 | 0.016 |
| YCSSQIDAEMRDILQS | YC[57.0215]SSQIDAEMRDILQS | R | - | 2C(57.0215) | VTDB * | 1267678.4 ± 111017.6 | 618448.7 ± 186918.9 | 0.005 |
| AKAYLEEECPTMLKK | AKAYLEEEC[57.0215]PTM[15.9949]LKK | R | Y | 12M(15.9949), 9C(57.0215) | ZA2G | 44553.7 ± 10736.4 | 0.0 ± 3913.5 | 0.007 |

*Indicates proteins not expressed in lungs. **Pyro-glutamate formation** from N-terminal glutamine (Q → pyro-Glu, −17.0265 Da), **Proline and Methionine oxidation** (+15.9949 Da), **Cysteine carbamidomethylation** (+57.0215 Da, a standard alkylation of cysteines (typically using iodoacetamide) to block free thiols and prevent artificial disulfide formation during sample prep).

**Table 3. Functions of Modified Proteins.**

| *Entry Name* | Proteins | Function | References |
|---|---|---|---|
| A1AT | Alpha-1-antiproteinase | acute-phase protein that inhibits the serine proteases, specifically, neutrophil elastase, proteinase, in the lungs | https://pubmed.ncbi.nlm.nih.gov/27564662/ |
| A1I3 | Alpha-1-inhibitor 3 | suppress overexpressed proteases during inflammation; oxidation of this protein can lead to an alteration of its activity | https://www.sciencedirect.com/topics/medicine-and-dentistry/alpha-1-antitrypsin |
| A1M | Alpha-1-macroglobulin | acts as a mediator of bacterial adhesion to polymer surfaces and is involved in inhibiting renal lithogenesis | https://www.sciencedirect.com/topics/medicine-and-dentistry/alpha-1-microglobulin |
| ACTC | Actin, alpha cardiac muscle 1 | plays an important role in heart development | https://pmc.ncbi.nlm.nih.gov/articles/PMC8698029/ |
| AL1A7 | Aldehyde dehydrogenase, cytosolic 1 | functional marker for identifying cancer stem cells in human nasopharyngeal carcinoma | https://www.ncbi.nlm.nih.gov/gene/216 |
| ALBU | Albumin | modulator of plasma oncotic pressure and transports various substances | https://www.ncbi.nlm.nih.gov/books/NBK459198/ |
| ALS | Insulin-like growth factor-binding protein complex acid labile subunit | important role in regulating the access of circulating IGFs to the tissues | https://www.ncbi.nlm.nih.gov/gene/3483 |

© 2026 by the author(s). Distributed under a Creative Commons CC BY license.

Preprints.org (www.preprints.org) | NOT PEER-REVIEWED | Posted: 18 September 2026 doi:10.20944/preprints202609.1607.v1



| | | | |
|---|---|---|---|
| ATRN | Attractin | plays a critical role in immune response, CNS development, and energy homeostasis | https://www.ncbi.nlm.nih.gov/gene/8455 |
| C4BPA | C4b-binding protein alpha chain | prevents uncontrolled activation of the classical and lectin complement pathways. | https://pmc.ncbi.nlm.nih.gov/articles/PMC10629839/ |
| CAP1 | Adenylyl cyclase-associated protein 1 | receptor for human resistin and mediates inflammatory actions of human monocytes | https://pubmed.ncbi.nlm.nih.gov/24606903/ |
| CATA | Catalase | antioxidant, scavenges $H_2O_2$ | https://pubmed.ncbi.nlm.nih.gov/16618987/ |
| CLUS | Clusterin | facilitates extracellular clearance of misfolded proteins | https://www.sciencedirect.com/science/article/pii/S0753332220313676 |
| CO4 | Complement C4 | inhibits human adenovirus infection by the deposition of cleaved C4b on capsid | https://pmc.ncbi.nlm.nih.gov/articles/PMC8317844/ |
| F13A* | Coagulation factor XIII A chain | catalyzes covalent cross-linking bonds between the $\alpha$ and $\gamma$ chains of fibrin polymer | https://www.sciencedirect.com/topics/medicine-and-dentistry/coagulation-factor-xiii#:~:text=Factor%20XIII%20assay-,Coagulation%20factor%20XIII%20is%20a%20transglutaminase%20that%20catalyzes%20covalent%20cross,%CE%B3%20chains%20of%20fibrin%20polymer.&text=Cross%2Dlinking%20strengthens%20the%20fibrin,renders%20it%20resistant%20to%20proteases. |
| FA12 | Coagulation factor XII | serum glycoprotein that participates in the initiation of blood coagulation, fibrinolysis, and the generation of bradykinin and angiotensin | https://pmc.ncbi.nlm.nih.gov/articles/PMC2851158/ |
| FA7* | Coagulation factor VII | single-chain glycoprotein synthesized in the liver, dependent on vitamin K, that plays a role in blood coagulation | https://www.sciencedirect.com/topics/neuroscience/factor-vii |
| FA9 | Coagulation factor IX | plays a role in blood coagulation | https://medlineplus.gov/genetics/gene/f9/ |
| FBLN3* | EGF-containing fibulin-like extracellular matrix protein 1 | maintain the stability of the basement membrane and the integrity of the extracellular matrix | https://onlinelibrary.wiley.com/doi/full/10.1002/cam4.2144 |
| FETUB | Fetuin-B | regulates TGFβ receptor-mediated Smad pathway in vascular smooth muscle cells, inflammation, and potential biomarker of COPD | https://www.ncbi.nlm.nih.gov/gene/26998 |
| FIBB | Fibrinogen beta chain | major function in hemostasis as one of the primary components of blood clots | https://www.sinobiological.com/resource/fibrinopeptide-b |
| FINC* | Fibronectin | functions in cell adhesion, migration, and differentiation, and regulates cell-matrix and matrix-matrix interactions | https://www.sciencedirect.com/topics/medicine-and-dentistry/fibronectin |
| HABP2 | Hyaluronan-binding protein 2 | negatively regulates vascular integrity via activation of PAR receptor/RhoA/ROCK signaling | https://www.ahajournals.org/doi/10.1161/atvbaha.109.200451 |
| HEMO* | Hemopexin | plasma protein with the highest binding affinity to heme among known proteins | https://pubmed.ncbi.nlm.nih.gov/12042069/ |

© 2026 by the author(s). Distributed under a Creative Commons CC BY license.

Preprints.org (www.preprints.org) | NOT PEER-REVIEWED | Posted: 18 September 2026 doi:10.20944/preprints202609.1607.v1



| | | | |
|---|---|---|---|
| HEP2 | Heparin cofactor 2 | plasma protein that inhibits thrombin rapidly in the presence of dermatan sulfate, heparan sulfate, or heparin | https://pmc.ncbi.nlm.nih.gov/articles/PMC150836/ |
| HPT* | Haptoglobin | bind free hemoglobin released from lysed erythrocytes and thus prevent the iron within hemoglobin from reacting with molecular oxygen to produce the free radical superoxide | https://www.sciencedirect.com/topics/agricultural-and-biological-sciences/haptoglobin#:~:text=Haptoglobin%20(Hp)%20is%20a%20hemoglobin,free%20radical%20superoxide%20%5B79%5D. |
| HRG | Histidine-rich glycoprotein | multivalent function in blood coagulation, fibrinolysis, and innate immune systems | https://pubmed.ncbi.nlm.nih.gov/23809442/ |
| IGF1* | Insulin-like growth factor 1 | manage the effects of growth hormone (GH) | https://pmc.ncbi.nlm.nih.gov/articles/PMC8534318/ |
| IGG2A* | Ig gamma-2A chain C region | interacts with Fc receptors on various immune cells, triggering processes like antibody-dependent cellular cytotoxicity (ADCC), phagocytosis, and complement activation | https://www.ncbi.nlm.nih.gov/gene/380793#:~:text=Summary,of%20Genome%20Resources%2C%20Jun%202025%5D |
| KACB* | Ig kappa chain C region, B allele | gene and protein expression in human non-small cell lung cancer is associated with prognosis | https://www.ncbi.nlm.nih.gov/gene?Db=gene&Cmd=DetailsSearch&Term=3514 |
| KLKB1 | Plasma kallikrein | enzyme that functions in the vascular space by liberating vasoactive peptides, such as bradykinin, from kininogens | https://www.sciencedirect.com/topics/neuroscience/plasma-kallikrein |
| KNG1* | Kininogen-1 | plays a crucial role in the kinin-kallikrein system, affecting blood coagulation, inflammation, and blood pressure | https://www.sciencedirect.com/topics/biochemistry-genetics-and-molecular-biology/kininogen |
| KPCA | Protein kinase C alpha type | family of serine–threonine kinases which has been shown to be involved in cell cycle, cellular processes, and apoptosis | https://www.sciencedirect.com/topics/medicine-and-dentistry/protein-kinase-c-alpha |
| LBP | Lipopolysaccharide-binding protein | modulate the innate immune response | https://www.sciencedirect.com/topics/biochemistry-genetics-and-molecular-biology/lipopolysaccharide-binding-protein |
| MASP2* | Mannan-binding lectin serine protease 2 | essential enzyme for the lectin pathway (LP) of complement activation | https://pmc.ncbi.nlm.nih.gov/articles/PMC5184842/ |
| MMP2 | 72 kDa type IV collagenase | a metalloproteinase thought to play a role in metastasis and in angiogenesis | https://www.sciencedirect.com/science/article/pii/S0021925819495471#:~:text=The%2072%2DkDa%20gelatinase%2Ftype,potent%20inhibitor%20of%20enzyme%20activity. |
| MUG1* | Murinoglobulin-1 | protease inhibitor that undergoes specific proteolytic activation, triggers conformational changes, and traps or covalently binds proteases | https://www.medchemexpress.com/recombinant-proteins/murinoglobulin-1-mug1-protein-mouse-his.html#:~:text=Murinoglobulin%2D1%20(Mug1)%20protein,hindrance%20alone%20provides%20strong%20inhibition. |
| MYH9* | Myosin-9 | participates in a variety of processes requiring the generation of intracellular chemomechanical force and translocation of the actin cytoskeleton | https://www.sciencedirect.com/science/article/pii/S0378111918304165 |
| PCSK9* | Proprotein convertase | important regulator of cholesterol metabolism | https://www.ncbi.nlm.nih.gov/books/NBK448100/ |

© 2026 by the author(s). Distributed under a Creative Commons CC BY license.

Preprints.org (www.preprints.org) | NOT PEER-REVIEWED | Posted: 18 September 2026 doi:10.20944/preprints202609.1607.v1



| | | | |
|---|---|---|---|
| | subtilisin/kexin type 9 | | |
| PLF4 | Platelet factor 4 | promote blood coagulation, this cytokine is involved in innate and adaptive immunity in events when platelets are activated in response to infections | https://pubmed.ncbi.nlm.nih.gov/33050376/#:~:text=Platelet%20factor%204%20(PF4%2C%20CXCL4,activated%20in%20response%20to%20infections. |
| PLMN | Plasminogen | activation results in increased conversion of plasminogen to plasmin | https://www.ncbi.nlm.nih.gov/books/NBK539745/ |
| PPIA | Peptidyl-prolyl cis-trans isomerase A | catalyze the cis-trans isomerization of peptide bonds N-terminal to proline residues, which is crucial for protein folding and function | https://www.ncbi.nlm.nih.gov/gene/5478 |
| PROC | Vitamin K-dependent protein C | serine protease that regulates blood coagulation by inactivating factors Va and VIIIa in the presence of calcium ions | https://www.sciencedirect.com/topics/medicine-and-dentistry/vitamin-k-dependent-protein |
| PSA6 | Proteasome subunit alpha type-6 | Component of the 20S core proteasome complex involved in the proteolytic degradation of most intracellular proteins | https://www.uniprot.org/uniprotkb/P60900/entry |
| SEPP1 | Selenoprotein P | selenium homeostasis and oxidant defense | https://pubmed.ncbi.nlm.nih.gov/16011466/ |
| SPA3K | Serine protease inhibitor A3K | Binds to and inhibits kallikreins. Inhibits trypsin but not chymotrypsin or elastase | https://pubmed.ncbi.nlm.nih.gov/23821192/ |
| SPA3N | Serine protease inhibitor A3N | regulates cardiac remodelling after myocardial infarction | https://www.ncbi.nlm.nih.gov/gene/20716 |
| THRB | Prothrombin | cleavage of fibrinogen into fibrin which ultimately results in the formation of a stable fibrin clot | https://www.sciencedirect.com/topics/medicine-and-dentistry/prothrombin |
| TRFE* | Serotransferrin | responsible for the transport of iron from sites of absorption and heme degradation to those of storage and utilization | https://olink.com/assay/explore/inflammation-ii/serotransferrin#:~:text=It%20is%20responsible%20for%20the,role%20in%20stimulating%20cell%20proliferation. |
| TSP4 | Thrombospondin-4 | promotes angiogenesis | https://pmc.ncbi.nlm.nih.gov/articles/PMC6005712/ |
| VCAM1 | Vascular cell adhesion protein 1 | helps regulate inflammation-associated vascular adhesion | https://www.nature.com/articles/s42003-023-04905-z |
| VTDB* | Vitamin D-binding protein | responsible for the transport of all vitamin D metabolites, which are therefore mainly protein bound | https://www.sciencedirect.com/topics/biochemistry-genetics-and-molecular-biology/vitamin-d-binding-protein |
| ZA2G | Zinc-alpha-2-glycoprotein | plays a significant role in multiple ways to regulate the fat mass of adipose tissue. It stimulates lipolysis, inhibits lipid accumulation in adipocytes, and regulates serum lipids by influencing adipokines | https://www.sciencedirect.com/org/science/article/pii/S032795452300186X#:~:text=Zinc%20Alpha%202%20Glycoprotein%20as,serum%20lipids%20by%20influencing%20adipokines. |

*Indicates proteins not expressed in lungs.

© 2026 by the author(s). Distributed under a Creative Commons CC BY license.

Preprints.org (www.preprints.org) | NOT PEER-REVIEWED | Posted: 18 September 2026 doi:10.20944/preprints202609.1607.v1



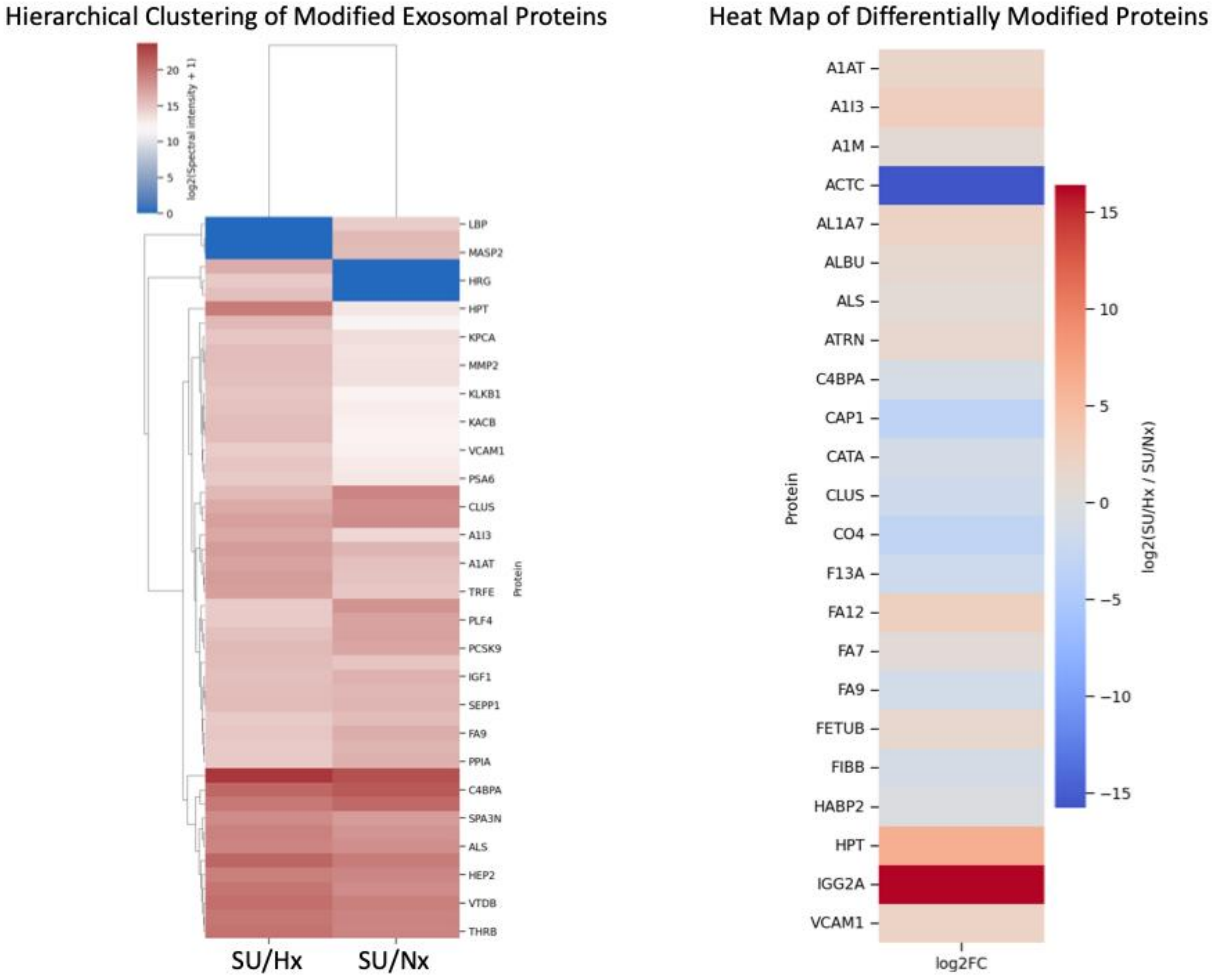


**Figure 5. Hierarchical clustering and differential enrichment of modified EV proteins in pulmonary hypertension. Left panel:** Hierarchical clustering heat map of post-translationally modified proteins identified in CD63⁺ EV isolated from blood collected from the left ventricle of SU/Hx and SU/Nx rats. Protein abundance is displayed as $\log_2$-transformed spectral intensity (+1), with red indicating higher and blue indicating lower relative abundance. Unsupervised clustering reveals distinct protein clusters enriched or diminished under hypoxic pulmonary hypertension conditions, highlighting coordinated regulation of EV cargo derived from lung and non-lung sources. **Right panel:** Heat map illustrating the $\log_2$ fold-change (SU/Hx vs. SU/Nx) of selected differentially modified EV proteins. Proteins such as HPT, IGG2A, VCAM1, and FETUB are markedly enriched in SU/Hx rats, whereas others (e.g., ACTC) are reduced, emphasizing condition-specific remodeling of EV protein cargo in experimental pulmonary hypertension.

**Functional mitochondria content is increased in EVs from rats with pulmonary hypertension:** Recent studies indicate that EV-mediated transfer of mitochondrial components can alter metabolic and inflammatory responses in recipient cells [19]. Deletion of the small GTPase Rab7 has been shown to increase secretion of EVs containing ubiquitinated cargo, including intact mitochondria [20]. Interestingly, in our study, Rab8A – an important regulator of intracellular vesicle trafficking and extracellular vesicle release – was decreased in EVs from SU/Hx rats, whereas several mitochondrial proteins, including long-chain fatty acid–CoA ligase 1, carbamoyl-phosphate synthase, glutamate dehydrogenase 1, and the 60-kDa heat shock protein, were increased compared with SU/Nx controls (Fig. 6A). These findings prompted us to assess mitochondrial content within the EVs. Representative forward and side scatter plots (Figure 6B), along with MitoGreen⁺ and MitoRed⁺ mitochondrial staining patterns (Figure 6C), are shown. Unexpectedly, EVs from SU/Hx rats exhibited an elevated MitoRed⁺/MitoGreen⁺ ratio indicates the presence of a greater abundance of functional mitochondria

© 2026 by the author(s). Distributed under a Creative Commons CC BY license.

Preprints.org (www.preprints.org) | NOT PEER-REVIEWED | Posted: 18 September 2026 doi:10.20944/preprints202609.1607.v1



with negative membrane potential in EVs from SU/Hx rats (Figure 6D). However, EVs from SU/Hx rats paradoxically exhibited reduced MitoSOX signal (Figure 6E).

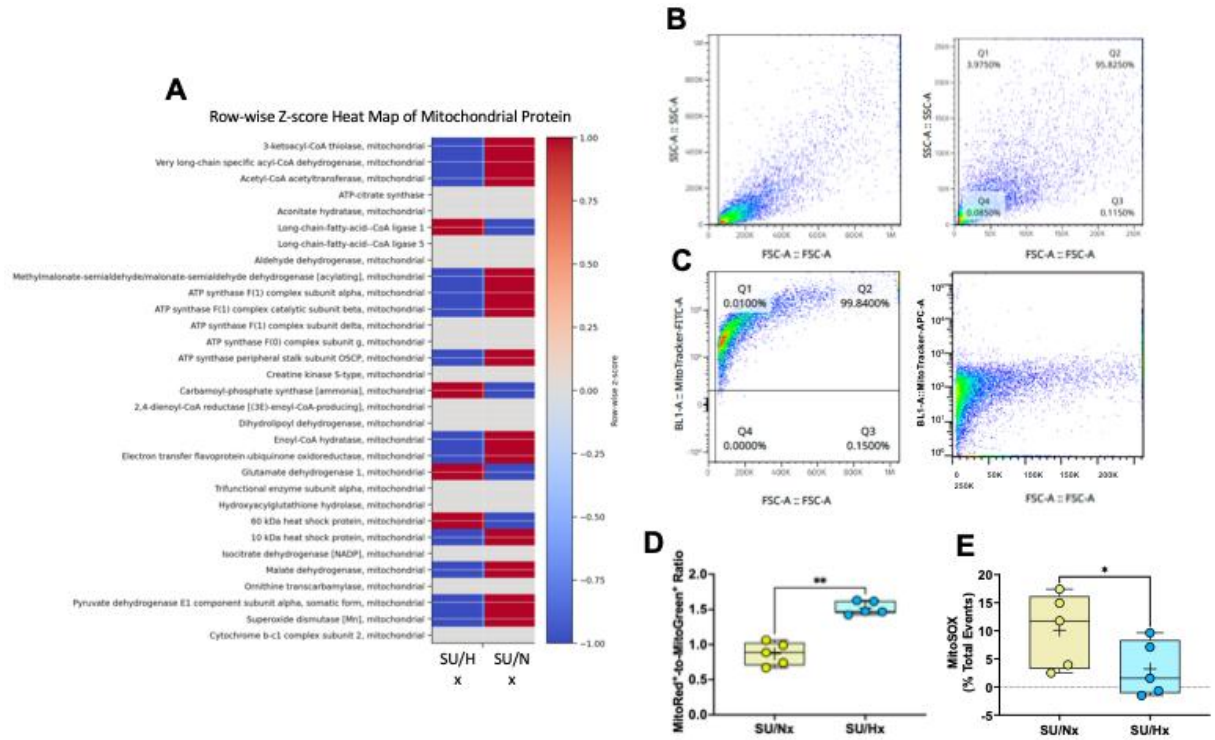


**Figure 6. EV mitochondrial protein enrichment and functional mitochondrial content are increased in SU/Hx rats.** (A) Row-wise *z*-score heat map of mitochondrial proteins identified by proteomic analysis in CD63⁺ EV isolated from blood collected from the left ventricle of SU/Hx and SU/Nx rats. Protein abundance is normalized across rows to highlight relative enrichment or depletion between conditions, with red indicating higher and blue indicating lower relative abundance. Multiple mitochondrial enzymes and chaperones are enriched in EV from SU/Hx rats. (B) Representative flow-cytometry forward scatter (FSC-A) *versus* side scatter (SSC-A) density plots showing the size and granularity of isolated EV prior to mitochondrial staining. (C) Representative flow-cytometry plots of EV stained with MitoTracker Green (total mitochondrial mass) and MitoTracker Red (mitochondria with intact membrane potential), gated on FSC-A *versus* fluorescence intensity. (D) Quantification of MitoGreen⁺ and MitoRed⁺ EV expressed as a percentage of total EV events in SU/Nx and SU/Hx groups. Ratio of MitoRed⁺ to MitoGreen⁺ EV, indicating an increased proportion of functionally active mitochondria within EV from SU/Hx rats. (E) Quantification of MitoSOX⁺ EVs expressed as a percentage of total EV events in the SU/Nx and SU/Hx groups. The proportion of MitoSOX⁺ EVs was significantly reduced in SU/Hx rats, indicating lower mitochondrial superoxide levels within EVs. Data are shown as individual data points with box-and-whisker plots. Statistical significance was determined using unpaired *t*-tests; **$p < 0.01$, ****$p < 0.0001$; ns, not significant.

## 3. Discussion

The findings of this study demonstrate that: EV levels in blood collected from the left ventricle are significantly higher in PH rats than in non-PH rats; EVs from PH rats carry and transmit both unmodified and post-translationally modified proteins and are enriched in functional mitochondria, while paradoxically exhibiting reduced superoxide anion levels, suggesting altered mitochondrial redox regulation.

PH is a multifactorial and multicellular disease [21]. Several animal models, including monocrotaline, hypoxia, and SU/Hx, have been used to investigate its pathogenesis [22]. Among these, the SU/Hx rat model is widely utilized because the pattern of pulmonary artery remodeling closely resembles that observed in human PH [22]. By isolating EVs from blood collected from the left ventricle and performing unbiased proteomic analyses to identify both unmodified and post-

© 2026 by the author(s). Distributed under a Creative Commons CC BY license.

Preprints.org (www.preprints.org) | NOT PEER-REVIEWED | Posted: 18 September 2026 doi:10.20944/preprints202609.1607.v1



translationally modified proteins, we determined that EV cargo carry lung- and liver-associated proteins are increased in SU/Hx rats (See Tables 2 and 3). Proteomic analysis revealed that EVs carried proteins with oxidation related post-translational modifications, including direct oxidation of methionine and proline residues, oxidation-induced deamidation of glutamine, and carbamidomethylation of cysteines. The +15.9949 Da mass shift commonly reflects the addition of a single oxygen atom and is most frequently attributed to oxidation of methionine (Met, M) and proline (Pro, P), representing both endogenous ROS (oxidative stress)-induced modifications and potential sample-preparation artifacts. Proline oxidation (+15.9949 Da) results in hydroxyproline formation, a modification commonly observed in collagen and frequently associated with fibrotic processes, which are known contributors to PH pathogenesis. Notably, increased oxidation of methionine (2.7:1.0 ratio) and proline (2.0:1.0 ratio) indicates a higher abundance of oxidized methionine- and proline-containing proteins in EVs from SU/Hx rats compared to SU/Nx rats. In contrast, higher cysteine carbamidomethylation (1.6:1.0 ratio; +57.0215 Da modification) – a standard alkylation of cysteine residues typically introduced during sample preparation using iodoacetamide to block free thiols and prevent artificial disulfide bond formation – suggests a higher abundance of reversibly oxidized cysteine residues in proteins from SU/Hx rats. Reduced cysteine residues are highly reactive and particularly susceptible to redox-dependent modifications [23]. The Q (-17.0265 Da) modification, often corresponding to N-terminal pyroglutamate formation, is a well-recognized PTM event that can substantially alter protein function by affecting charge, hydrogen bonding, and susceptibility to proteolytic degradation. N-terminal pyroglutamate formation removes the primary amine, protecting proteins from aminopeptidase-mediated degradation and playing a critical role in the maturation and stability of several hormones, cytokines, and neuropeptides, including neurotensin. This modification may also influence protein folding and intermolecular interactions by eliminating a hydrogen bond donor. The higher glutamine modification ratio (3.0:1.0) observed in SU/Hx rats indicates increased accumulation of pyroglutamate residues in EV proteins. Collectively, these potentially oxidative stress-dependent and oxidative stress-independent modifications of methionine, proline, cysteine, and glutamine suggest that SU/Hx exposure significantly alters the molecular composition and potential functionality of EV proteins in rats.

Our findings demonstrate that EV cargo from SU/Hx rats is enriched in a distinct cluster of both lung- and non-lung-associated proteins, including both unmodified proteins and proteins bearing redox-dependent and -independent post-translational modifications (e.g., HPT, IGG2A, VCAM1, and FETUB). Notably, HMGB1, a chromatin-associated DNA-binding protein that can also function extracellularly as a potent pro-inflammatory damage-associated molecular pattern (DAMP), was significantly enriched in SU/Hx EVs despite the absence of detectable PTMs. In addition to proteins linked to pulmonary vascular pathology, EVs contained numerous proteins of extrapulmonary origin, including coagulation factors and proteins involved in basement membrane maintenance, extracellular matrix organization, cell-matrix and matrix-matrix interactions, heme binding, growth hormone signaling, antibody-dependent cellular cytotoxicity, phagocytosis, complement activation, lectin pathway activation, protease inhibition, and pathways associated with non-small-cell lung cancer. In contrast, a reciprocal cluster of proteins, including CO4, CAP1, CLUS, and PLF4, was markedly reduced in SU/Hx EVs but abundant in SU/Nx controls, suggesting either diminished expression, impaired packaging, or selective exclusion of these proteins under hypoxic pulmonary hypertensive conditions. A separate cluster comprising highly abundant circulating proteins, such as MUG1, VTDB, and THRB, formed an independent branch within the clustering analysis, indicating that their segregation was primarily driven by overall abundance rather than disease-specific regulation. Functional annotation revealed that EV-associated proteins and PTMs collectively participate in biological pathways central to pulmonary hypertension pathogenesis, including inflammation, cell adhesion, vascular smooth muscle cell phenotypic switching, angiogenesis, coagulation, cardiac remodeling, innate immune activation, cell-cycle regulation, apoptosis, PAR and Rho/ROCK signaling, and metabolic homeostasis [24–26]. Collectively, these findings support the concept that SU/Hx-induced PH is associated with extensive remodeling of the circulating EV proteome and PTM landscape. The presence of EV cargo derived from both pulmonary and systemic

© 2026 by the author(s). Distributed under a Creative Commons CC BY license.

Preprints.org (www.preprints.org) | NOT PEER-REVIEWED | Posted: 18 September 2026 doi:10.20944/preprints202609.1607.v1



tissues suggests that EVs may serve as integrative mediators of interorgan communication, facilitating vascular remodeling, inflammatory signaling, immune dysregulation, and systemic pathophysiological responses that contribute to disease progression. These results further support growing evidence that PH is a systemic disorder characterized by widespread molecular and vascular abnormalities extending beyond the pulmonary circulation [27].

EVs released from diseased donor cells or organs can transmit biological materials to healthy recipient cells and organs [2]. Therefore, it is reasonable to propose that EVs carrying both unmodified and post-translationally modified proteins contribute to the inflammation and cardiac remodeling observed in SU/Hx-exposed rats. In addition, EVs transporting proteins that promote inflammation, vascular smooth muscle cell dedifferentiation, and hypoxia-induced intra-pulmonary fibrosis [10,28,29], are likely to trigger and remodeling of the vasculature and potentially other organs. Because non-lung proteins associated with coagulation and complement activation were elevated in SU/Hx rats, these EVs may also promote blood clot formation and activate immune pathways that drive systemic inflammation. Although the mechanism by which non-lung proteins (primarily liver-associated) enter circulating EVs remains unclear, PH is well known to impair liver function through venous congestion, which reduces oxygen delivery and disrupts hepatic synthetic activity [30]. Collectively, these findings suggest that both lung-derived and non-lung-derived EV cargo can potentially influence organ function, including vascular function, beyond the lungs.

Next, using flow cytometry, we found that circulating EVs isolated from blood collected from the left ventricle contain active mitochondria, as detected by labeling with mitochondria-specific dyes. MitoTracker Green labels total mitochondrial mass independently of membrane potential, whereas MitoTracker Red selectively stains healthy, functional mitochondria with an intact negative membrane potential. Interestingly, the increased ratio of MitoTracker Red$^{+}$ to MitoTracker Green$^{+}$ mitochondria in SU/Hx rats suggests a greater abundance of highly active mitochondria with strongly negative membrane potentials ($\Delta\Psi m \approx -140$ to $-180$ mV), indicating a relative enrichment of functionally active mitochondria. Such hyperpolarized mitochondria are typically associated with enhanced electron retention and increased electron leak from Complex I and Complex III of the electron transport chain, processes that can promote reactive oxygen species generation. Paradoxically, EVs from SU/Hx rats exhibited reduced MitoSOX fluorescence despite evidence of increased mitochondrial activity. This observation suggests that enhanced mitochondrial function within EVs is not necessarily accompanied by increased mitochondrial superoxide accumulation and may instead reflect reduced localized superoxide production or changes in MitoSOX probe accessibility, uptake, or retention. Nevertheless, because other ROS-generating pathways implicated in PH, such as NADPH oxidases and xanthine oxidase, were not evaluated, increased ROS production from non-mitochondrial sources cannot be ruled out. Supporting the presence of metabolically active and redox-sensitive cargo within EVs, proteomic analyses identified mitochondrial metabolic enzymes as well as proteins associated with the endoplasmic reticulum, nucleus, and peroxisomes, suggesting that EVs may serve as vehicles for inter-organellar signaling and redox regulation during PH progression. Although EVs are known to transport mitochondrial material [19,20,31], and EV – mediated mitochondrial trafficking may represent an additional mechanism for mitochondrial exchange distinct from direct cell – cell pore formation via connexin-43, as observed between hematopoietic stem cells and bone marrow fibroblasts [32,33], it has remained unclear whether EVs carry functional mitochondria in the context of PH. To the best of our knowledge, this study provides the first evidence that EVs in PH may contain functional mitochondria – or at least intact, metabolically active mitochondrial components. However, whether these mitochondria originate from the lungs, the liver, or both remains to be determined. Furthermore, the effects of functional or partially functional mitochondria on organ-level physiology, whole-body metabolism, and immune responses remain to be fully elucidated. Because mitochondria are evolutionary descendants of bacteria under the endosymbiotic theory, the presence of mitochondrial nucleic acids in the circulation could activate cGAS – STING-interferon signaling, promoting inflammation and the synthesis of immunomodulatory metabolites such as kynurenine – a pathway implicated in PH and SARS-CoV-2-associated pulmonary complications [34–40].

© 2026 by the author(s). Distributed under a Creative Commons CC BY license.

Preprints.org (www.preprints.org) | NOT PEER-REVIEWED | Posted: 18 September 2026 doi:10.20944/preprints202609.1607.v1



Consequently, mitochondria derived from diseased lungs may contribute to increased systemic oxidative stress, thereby elevating the risk of inflammation and damage in peripheral tissues and organs.

In conclusion, using an unbiased proteomic approach, we demonstrate that EV abundance is increased in this experimental model of PH. These EVs carry lung- and liver-associated proteins that may contribute to immune activation, inflammation, coagulation, and cardiac remodeling. In addition, EVs from PH rats contain a greater abundance of functional mitochondria.

**Limitation**: Although our study demonstrates increased levels of lung- and liver-associated proteins and mitochondria in circulating EVs, the precise cellular and tissue origins of these cargo components remain unclear and warrant further investigation.

## References


1. **Kumar MA, Baba SK, Sadida HQ, Marzooqi SA, Jerobin J, Altemani FH, Algehainy N, Alanazi MA, Abou-Samra AB, Kumar R, Al-Shabeeb Akil AS, Macha MA, Mir R, and Bhat AA**. Extracellular vesicles as tools and targets in therapy for diseases. *Signal Transduct Target Ther* 9: 27, 2024.
2. **Tkach M, and Thery C**. Communication by Extracellular Vesicles: Where We Are and Where We Need to Go. *Cell* 164: 1226–1232, 2016.
3. **Witwer KW, and Thery C**. Extracellular vesicles or exosomes? On primacy, precision, and popularity influencing a choice of nomenclature. *J Extracell Vesicles* 8: 1648167, 2019.
4. **Chiaradia E, Tancini B, Emiliani C, Delo F, Pellegrino RM, Tognoloni A, Urbanelli L, and Buratta S**. Extracellular Vesicles under Oxidative Stress Conditions: Biological Properties and Physiological Roles. *Cells* 10: 2021.
5. **Conti M, Minniti M, Tine M, De Francesco M, Gaeta R, Nieri D, Semenzato U, Biondini D, Camera M, Cosio MG, Saetta M, Celi A, Bazzan E, and Neri T**. Extracellular Vesicles in Pulmonary Hypertension: A Dangerous Liaison? *Biology (Basel)* 12: 2023.
6. **Sayner SL, Choi CS, Maulucci ME, Ramila KC, Zhou C, Scruggs AK, Yarbrough T, Blair LA, King JA, Seifert R, Kaever V, and Bauer NN**. Extracellular vesicles: another compartment for the second messenger, cyclic adenosine monophosphate. *Am J Physiol Lung Cell Mol Physiol* 316: L691–L700, 2019.
7. **Lammi MR, Saketkoo LA, Okpechi SC, Ghonim MA, Wyczechowska D, Bauer N, Pyakurel K, Saito S, deBoisblanc BP, and Boulares AH**. Microparticles in systemic sclerosis: Potential pro-inflammatory mediators and pulmonary hypertension biomarkers. *Respirology* 24: 675–683, 2019.
8. **D'Addario CA, Lanier GM, Jacob C, Bauer N, Hewes JL, Bhadra A, and Gupte SA**. Differences in the expression of DNA methyltransferases and demethylases in leukocytes and the severity of pulmonary arterial hypertension between ethnic groups. *Physiol Rep* 10: e15282, 2022.
9. **Blair LA, Haven AK, and Bauer NN**. Circulating microparticles in severe pulmonary arterial hypertension increase intercellular adhesion molecule-1 expression selectively in pulmonary artery endothelium. *Respir Res* 17: 133, 2016.
10. **Khandagale A, Aberg M, Wikstrom G, Bergstrom Lind S, Shevchenko G, Bjorklund E, Siegbahn A, and Christersson C**. Role of Extracellular Vesicles in Pulmonary Arterial Hypertension: Modulation of Pulmonary Endothelial Function and Angiogenesis. *Arterioscler Thromb Vasc Biol* 40: 2293–2309, 2020.
11. **Hogan SE, Rodriguez Salazar MP, Cheadle J, Glenn R, Medrano C, Petersen TH, and Ilagan RM**. Mesenchymal stromal cell-derived exosomes improve mitochondrial health in pulmonary arterial hypertension. *Am J Physiol Lung Cell Mol Physiol* 316: L723–L737, 2019.
12. **Hewes JL, and Bauer NN**. Extracellular vesicles in pulmonary hypertension: lessons from mesenchymal stromal cell-derived exosomes. *Am J Physiol Lung Cell Mol Physiol* 316: L720–L722, 2019.
13. **Abe K, Toba M, Alzoubi A, Ito M, Fagan KA, Cool CD, Voelkel NF, McMurtry IF, and Oka M**. Formation of plexiform lesions in experimental severe pulmonary arterial hypertension. *Circulation* 121: 2747–2754, 2010.
14. **de Brito Monteiro L, Davanzo GG, de Aguiar CF, Correa da Silva F, Andrade JR, Campos Codo A, Silva Pereira JAD, Freitas LP, and Moraes-Vieira PM**. M-CSF- and L929-derived macrophages present distinct metabolic profiles with similar inflammatory outcomes. *Immunobiology* 225: 151935, 2020.


© 2026 by the author(s). Distributed under a Creative Commons CC BY license.

Preprints.org (www.preprints.org) | NOT PEER-REVIEWED | Posted: 18 September 2026 doi:10.20944/preprints202609.1607.v1




15. **Jacob C, Kitagawa A, Signoretti C, Dzieciatkowska M, D'Alessandro A, Gupte A, Hossain S, D'Addario CA, Gupte R, and Gupte SA**. Mediterranean G6PD variant mitigates expression of DNA methyltransferases and right heart pressure in experimental model of pulmonary hypertension. *J Biol Chem* 298: 102691, 2022.
16. **Dzieciatkowska M, Hill R, and Hansen KC**. GeLC-MS/MS analysis of complex protein mixtures. *Methods Mol Biol* 1156: 53–66, 2014.
17. **Joshi SR, Kitagawa A, Jacob C, Hashimoto R, Dhagia V, Ramesh A, Zheng C, Zhang H, Jordan A, Waddell I, Leopold J, Hu CJ, McMurtry IF, D'Alessandro A, Stenmark KR, and Gupte SA**. Hypoxic activation of glucose-6-phosphate dehydrogenase controls the expression of genes involved in the pathogenesis of pulmonary hypertension through the regulation of DNA methylation. *Am J Physiol Lung Cell Mol Physiol* 318: L773–L786, 2020.
18. **Tabima DM, Frizzell S, and Gladwin MT**. Reactive oxygen and nitrogen species in pulmonary hypertension. *Free Radic Biol Med* 52: 1970–1986, 2012.
19. **Amari L, and Germain M**. Mitochondrial Extracellular Vesicles - Origins and Roles. *Front Mol Neurosci* 14: 767219, 2021.
20. **Liang W, Sagar S, Ravindran R, Najor RH, Quiles JM, Chi L, Diao RY, Woodall BP, Leon LJ, Zumaya E, Duran J, Cauvi DM, De Maio A, Adler ED, and Gustafsson AB**. Mitochondria are secreted in extracellular vesicles when lysosomal function is impaired. *Nat Commun* 14: 5031, 2023.
21. **Wilkins MR**. Pulmonary hypertension: the science behind the disease spectrum. *Eur Respir Rev* 21: 19–26, 2012.
22. **Stenmark KR, Meyrick B, Galie N, Mooi WJ, and McMurtry IF**. Animal models of pulmonary arterial hypertension: the hope for etiological discovery and pharmacological cure. *Am J Physiol Lung Cell Mol Physiol* 297: L1013–1032, 2009.
23. **Marino SM, and Gladyshev VN**. Analysis and functional prediction of reactive cysteine residues. *J Biol Chem* 287: 4419–4425, 2012.
24. **Humbert M, Morrell NW, Archer SL, Stenmark KR, MacLean MR, Lang IM, Christman BW, Weir EK, Eickelberg O, Voelkel NF, and Rabinovitch M**. Cellular and molecular pathobiology of pulmonary arterial hypertension. *J Am Coll Cardiol* 43: 13S–24S, 2004.
25. **D'Alessandro A, El Kasmi KC, Plecita-Hlavata L, Jezek P, Li M, Zhang H, Gupte SA, and Stenmark KR**. Hallmarks of Pulmonary Hypertension: Mesenchymal and Inflammatory Cell Metabolic Reprogramming. *Antioxid Redox Signal* 28: 230–250, 2018.
26. **Stenmark KR, Fagan KA, and Frid MG**. Hypoxia-induced pulmonary vascular remodeling: cellular and molecular mechanisms. *Circ Res* 99: 675–691, 2006.
27. **Nickel NP, Yuan K, Dorfmuller P, Provencher S, Lai YC, Bonnet S, Austin ED, Koch CD, Morris A, Perros F, Montani D, Zamanian RT, and de Jesus Perez VA**. Beyond the Lungs: Systemic Manifestations of Pulmonary Arterial Hypertension. *Am J Respir Crit Care Med* 201: 148–157, 2020.
28. **Alvarado-Vasquez N, Rangel-Escareno C, de Jesus Ramos-Abundis J, Becerril C, and Negrete-Garcia MC**. The possible role of hypoxia-induced exosomes on the fibroblast metabolism in idiopathic pulmonary fibrosis. *Biomed Pharmacother* 181: 117680, 2024.
29. **Su SA, Xie Y, Fu Z, Wang Y, Wang JA, and Xiang M**. Emerging role of exosome-mediated intercellular communication in vascular remodeling. *Oncotarget* 8: 25700–25712, 2017.
30. **Nickel NP, Galura GM, Zuckerman MJ, Hakim MN, Alkhateeb H, Mukherjee D, Austin ED, and Heresi GA**. Liver abnormalities in pulmonary arterial hypertension. *Pulm Circ* 11: 20458940211054304, 2021.
31. **Corssac GB, Bonetto JP, Campos-Carraro C, Cechinel LR, Zimmer A, Parmeggiani B, Grings M, Carregal VM, Massensini AR, Siqueira I, Leipnitz G, and Bello-Klein A**. Pulmonary arterial hypertension induces the release of circulating extracellular vesicles with oxidative content and alters redox and mitochondrial homeostasis in the brains of rats. *Hypertens Res* 44: 918–931, 2021.
32. **Taniguchi Ishikawa E, Gonzalez-Nieto D, Ghiaur G, Dunn SK, Ficker AM, Murali B, Madhu M, Gutstein DE, Fishman GI, Barrio LC, and Cancelas JA**. Connexin-43 prevents hematopoietic stem cell senescence through transfer of reactive oxygen species to bone marrow stromal cells. *Proc Natl Acad Sci U S A* 109: 9071–9076, 2012.


© 2026 by the author(s). Distributed under a Creative Commons CC BY license.

Preprints.org (www.preprints.org) | NOT PEER-REVIEWED | Posted: 18 September 2026 doi:10.20944/preprints202609.1607.v1




33. **Peruzzotti-Jametti L, Bernstock JD, Willis CM, Manferrari G, Rogall R, Fernandez-Vizarra E, Williamson JC, Braga A, van den Bosch A, Leonardi T, Krzak G, Kittel A, Beninca C, Vicario N, Tan S, Bastos C, Bicci I, Iraci N, Smith JA, Peacock B, Muller KH, Lehner PJ, Buzas EI, Faria N, Zeviani M, Frezza C, Brisson A, Matheson NJ, Viscomi C, and Pluchino S**. Neural stem cells traffic functional mitochondria via extracellular vesicles. *PLoS Biol* 19: e3001166, 2021.
34. **Murphy MP, and O'Neill LAJ**. A break in mitochondrial endosymbiosis as a basis for inflammatory diseases. *Nature* 626: 271–279, 2024.
35. **Kim J, Kim HS, and Chung JH**. Molecular mechanisms of mitochondrial DNA release and activation of the cGAS-STING pathway. *Exp Mol Med* 55: 510–519, 2023.
36. **Nemkov T, Stephenson D, Erickson C, Dzieciatkowska M, Key A, Moore A, Earley EJ, Page GP, Lacroix IS, Stone M, Deng X, Raife T, Kleinman S, Zimring JC, Roubinian N, Hansen KC, Busch MP, Norris PJ, and D'Alessandro A**. Regulation of kynurenine metabolism by blood donor genetics and biology impacts red cell hemolysis in vitro and in vivo. *Blood* 143: 456–472, 2024.
37. **Nagy BM, Nagaraj C, Meinitzer A, Sharma N, Papp R, Foris V, Ghanim B, Kwapiszewska G, Kovacs G, Klepetko W, Pieber TR, Mangge H, Olschewski H, and Olschewski A**. Importance of kynurenine in pulmonary hypertension. *Am J Physiol Lung Cell Mol Physiol* 313: L741–L751, 2017.
38. **Cai Z, Tian S, Klein T, Tu L, Geenen LW, Koudstaal T, van den Bosch AE, de Rijke YB, Reiss IKM, Boersma E, van der Ley C, Van Faassen M, Kema I, Duncker DJ, Boomars KA, Tran-Lundmark K, Guignabert C, and Merkus D**. Kynurenine metabolites predict survival in pulmonary arterial hypertension: A role for IL-6/IL-6Ralpha. *Sci Rep* 12: 12326, 2022.
39. **Thomas T, Stefanoni D, Reisz JA, Nemkov T, Bertolone L, Francis RO, Hudson KE, Zimring JC, Hansen KC, Hod EA, Spitalnik SL, and D'Alessandro A**. COVID-19 infection alters kynurenine and fatty acid metabolism, correlating with IL-6 levels and renal status. *JCI Insight* 5: 2020.
40. **D'Alessandro A, Thomas T, Akpan IJ, Reisz JA, Cendali FI, Gamboni F, Nemkov T, Thangaraju K, Katneni U, Tanaka K, Kahn S, Wei AZ, Valk JE, Hudson KE, Roh D, Moriconi C, Zimring JC, Hod EA, Spitalnik SL, Buehler PW, and Francis RO**. Biological and Clinical Factors Contributing to the Metabolic Heterogeneity of Hospitalized Patients with and without COVID-19. *Cells* 10: 2021.


**Disclaimer/Publisher's Note:** The statements, opinions and data contained in all publications are solely those of the individual author(s) and contributor(s) and not of MDPI and/or the editor(s). MDPI and/or the editor(s) disclaim responsibility for any injury to people or property resulting from any ideas, methods, instructions or products referred to in the content.

© 2026 by the author(s). Distributed under a Creative Commons CC BY license.